International Journal of Infectious Diseases 103 (2021) 628–635

Contents lists available at ScienceDirect

International Journal of Infectious Diseases

journal homepage: www.elsevier.com/locate/ijid

B cell depletion and signs of sepsis-acquired immunodeficiency in bone marrow and spleen of COVID-19 deceased

Jana Ihlow[a,*], Edward Michaelis[a], Selina Greuel[a], Verena Heynol[a], Annika Lehmann[a], Helena Radbruch[c], Jenny Meinhardt[c], Florian Miller[d], Hermann Herbst[d], Victor Max Corman[e], Jörg Westermann[b], Lars Bullinger[b], David Horst[a,1], Ann-Christin von Brünneck[a,1], Sefer Elezkurtaj[a,1]

[a] Institute of Pathology, Charité – Universitätsmedizin Berlin, corporate member of Freie Universität Berlin, Humboldt-Universität zu Berlin, and Berlin Institute of Health, Berlin, Germany
[b] Department of Hematology, Oncology and Tumor Immunology, Charité – Universitätsmedizin Berlin, Campus Virchow-Clinic, corporate member of Freie Universität Berlin and Humboldt-Universität zu Berlin, and Berlin Institute of Health, Germany
[c] Institute of Neuropathology, Charité – Universitätsmedizin Berlin, corporate member of Freie Universität Berlin, Humboldt-Universität zu Berlin, and Berlin Institute of Health, Berlin, Germany
[d] Department of Pathology, Vivantes Netzwerk für Gesundheit GmbH, Berlin, Germany
[e] Institute of Virology, Charité – Universitätsmedizin Berlin, corporate member of Freie Universität Berlin and Humboldt-Universität zu Berlin, Berlin Institute of Health, and German Centre for Infection Research, Berlin, Germany

ARTICLE INFO

Article history:
Received 24 November 2020
Received in revised form 24 December 2020
Accepted 28 December 2020

Keywords:
COVID-19
SARS-CoV-2
Bone marrow
Spleen
B cells
Sepsis
Immunodeficiency
Humoral immune response

ABSTRACT

Objectives: In coronavirus disease 2019 (COVID-19), the adaptive immune response is of considerable importance, and detailed cellular immune reactions in the hematological system of patients with severe acute respiratory syndrome coronavirus 2 (SARS-CoV-2) infection are yet to be clarified.
Methods: This study reports the morphological characterization of both bone marrow and spleen in 11 COVID-19 decedents with respect to findings in the peripheral blood and pulmonary SARS-CoV-2 burden.
Results: In the bone marrow, activation and left shift were found in at least 55% of patients, which was mirrored by peripheral anaemia, granulocytic immaturity and multiple thromboembolic events. Signs of sepsis-acquired immunodeficiency were found in the setting of an abscess-forming superinfection of viral COVID-19 pneumonia. Furthermore, a severe B cell loss was observed in the bone marrow and/or spleen in 64% of COVID-19 patients. This was reflected by lymphocytopenia in the peripheral blood. As compared to B cell preservation, B cell loss was associated with a higher pulmonary SARS-CoV-2 burden and only a marginal decrease of of T cell counts.
Conclusions: The results of this study suggest the presence of sepsis-related immunodeficiency in severe COVID-19 pneumonia with superinfection. Furthermore, our findings indicate that lymphocytopenia in COVID-19 is accompanied by B cell depletion in hematopoietic tissue, which might impede the durability of the humoral immune response to SARS-CoV-2.

Introduction

Over the past months, the pandemic spread of severe acute respiratory syndrome coronavirus 2 (SARS-CoV-2) has claimed more than 1.5 million lives (WHO, 2020). Current mortality rates with severe coronavirus disease 2019 (COVID-19) are approximately 5%, which is relatively high as compared to death from influenza (Faust and del Rio, 2020; Iuliano et al., 2018; WHO, 2020). Although pulmonary factors such as diffuse alveolar damage and pneumonia are major immediate causes of death in patients with COVID-19, recent studies have proposed that endotheliitis and thromboses contribute to the severity of pulmonary damage (Ackermann et al., 2020; Bryce et al., 2020; Lax et al., 2020; Levi et al., 2020; Varga et al., 2020). Nevertheless, the deduction of therapeutic algorithms from this knowledge is difficult. This reflects the heterogeneity of the clinical outcomes of SARS-CoV-2 infection.

* Corresponding author at: Institute of Pathology, Charité–Universitätsmedizin Berlin, Charitéplatz 1, 10117 Berlin, Germany.
E-mail address: jana.ihlow@charite.de (J. Ihlow).
[1] David Horst, Ann-Christin von Brünneck, and Sefer Elezkurtaj contributed equally.

https://doi.org/10.1016/j.ijid.2020.12.078

With regard to the pathophysiology of COVID-19, T cell-mediated immunity seems to play a major role, which has been linked to severe lymphocytopenia in the blood (Terpos et al., 2020; Zheng et al., 2020). Recent findings also indicate a T cell-mediated germinal centre atrophy in the lymph node and the spleen with loss of germinal centre B cells in early COVID-19 (Kaneko et al., 2020). However, it is unclear whether bone marrow B cells are affected by the systemic invasion of SARS-CoV-2.

This study reports a post-mortem analysis of bone marrow and splenic tissue in patients who died of COVID-19, which contributes substantially to recent findings on the pathogenesis and adds further explanation regarding the lack of a durable immune response in SARS-CoV-2 infection.

Materials and methods

Study design

Post-mortem examinations were performed on a total of 15 patients. Eleven of these patients had PCR-confirmed SARS-CoV-2 infection and were diagnosed with COVID-19. The remaining four patients had died from cardiac conditions and were matched for age, thereby serving as a control group. On the legal basis of §1 SRegG BE of the autopsy act of Berlin and §25 of the German Infection Protection Act, autopsies were either performed at Charité University Medical Centre Berlin or at Vivantes Hospitals Berlin. The study was performed in accordance with local ethics guidelines (ethics committee approval EA2/066/20) and the Declaration of Helsinki. Written consent was obtained from all next of kin. Clinical data were obtained from the clinical records or death certificates.

Autopsy procedure

A complete autopsy was performed in 11 patients with COVID-19 and four control patients. Proper safety precautions were undertaken and the autopsies were performed in an enclosed space according to the safety guidelines (CDC, 2020). Pulmonary samples, bone marrow from vertebral bodies, and splenic tissue were obtained for histopathology.

Sample preparation and assessment

Bone marrow and spleen samples were fixed in formalin and the bone marrow was then decalcified with a solution of 20% ethylenediaminetetraacetic acid (EDTA) for 8 h overnight. The samples were then dehydrated and embedded in paraffin. Sections of paraffin-embedded bone marrow and spleen were stained with haematoxylin–eosin (HE), periodic acid–Schiff stain (PAS), Giemsa, Gomori, and Prussian blue stains. Additionally, immunohistochemical staining was performed according to standard protocols provided by the LEICA Bond III, LEICA Bond MAX (Leica Biosystems, Buffalo, NY, USA) or the automated Ventana BenchMark XT immunostainer (Ventana Medical Systems, Inc., Tucson, AZ, USA). Briefly, the tissue sections were deparaffinized, rehydrated, and subjected to heat-induced epitope retrieval and endogenous peroxidase blocking with H_2O_2. Subsequently, bone marrow slides were incubated for 30 min with the following primary antibodies and the indicated dilutions: CD235 (1:400, Dako), myeloperoxidase (MPO, 1:3000, Dako), CD34 (1:50, Leica), CD117 (1:400, Dako), CD68 (1:200, Dako), CD61 (1:100, Leica), CD20 (1:750, Dako), CD3 (1:100, Dako), CD4 (1:20, Leica), CD8 (1:100, Dako), CD138 (1:25, Dako), human leukocyte antigen isotype DR (HLA-DR, 1:25, Leica), programmed cell death protein and ligand 1 (PD-1, 1:100, Epitomics; PD-L1, 1:200, Cell Signaling), or caspase 3 (1:400, Zytomed). A horseradish peroxidase (HRP)-conjugated secondary antibody (Leica) then was applied for 32 min. In the same manner, the spleen slides were stained with primary antibodies against Ki67 (1:100, Dako), CD20, CD3, CD4, CD8, CD3, CD34, CD61, CD68, HLA-DR, and PD-L1. This was followed by chromogen 3,3′-diaminobenzidine tetrahydrochloride (DAB) application for 8 min and counterstaining with haematoxylin (Ventana and Leica Bond) and bluing reagent (Ventana only) for 12 min. All slides were examined with a Leica DMLB microscope and a 40× ocular lens (field number 25) by at least two haematopathologists. In the bone marrow, quantification of cell types and apoptosis was performed by minimum counts of 10 high-power fields (HPF). The bone marrow evaluation was conducted in analogy to morphological assessment of iliac trephine biopsies (Tzankov et al., 2012). In splenic tissue, cells were counted as percentage of specimen surface. Immunohistochemical expression was classified by the percentage of stained cells and staining intensity, which were graded as either strong, moderate, weak, or absent.

Epstein–Barr virus in situ hybridization and PCR

For the bone marrow samples, Epstein–Barr virus (EBV)-encoded ribonucleic acid (EBER RNA) in situ hybridization (ISH) was performed using the automated Leica Bond III System in combination with anti-fluorescein antibodies and the BOND Polymer refine detection system, consisting of HRP conjugated anti-rabbit antibodies. 3,3′-DAB was used as chromogen for visualization. Finally, the slides were counterstained with haematoxylin.

As control for the EBER-ISH results, PCR was performed for the determination of the viral EBV load. Deoxyribonucleic acid (DNA) was extracted from biopsy specimens using the Maxwell RSC DNA FFPE Kit (Promega). Subsequently, a conserved region of the human EBV nuclear antigen 1 gene (EBNA1, BKRF1) was amplified using ReddyMix PCR Master Mix (Thermo Fisher Scientific), a PCR digoxigenin labelling mix (PCR DIG Labeling Mix, Roche), and a mix of Epstein–Barr 30 and Epstein–Barr 40 primers.

SARS-CoV-2-specific PCR and subgenomic RNA assessment in pulmonary tissue

Fifty milligrams of pulmonary tissue from each COVID patient was homogenized. RNA was subsequently purified using the MagNA Pure 96 system and the MagNA Pure 96 DNA and Viral NA Large Volume Kit (Roche) following the manufacturer's instructions. The RNA extracts were used for quantitative real-time PCR targeting the SARS-CoV-2 E-gene. Viral RNA was quantified by in vitro RNA transcripts that had been photometrically quantified prior to the study. Total DNA was measured in all extracts using the Qubit dsDNA HS Assay Kit (Thermo Fisher Scientific). Detection of subgenomic RNA (sgRNA) was performed using oligonucleotides targeting the leader transcriptional regulatory sequence and region within the sgRNA coding for the E-gene, as described previously (Wölfel et al., 2020).

Statistical analysis

The data collection and statistical analysis were performed using IBM SPSS Statistics version 23 (2017; IBM Corp., Armonk, NY, USA) and GraphPad Prism 8 (2018; GraphPad Software, Inc.). Comparisons between dichotomous groups were performed using the Fisher's exact test or Chi-square test. The time from onset to death was analysed using the Kaplan–Meier method.

Results

Causes of death in patients with COVID-19

Autopsies were performed on 11 patients with COVID-19-initiated death and four control patients who died from cardiac

Table 1
Characteristics, treatment, and major autopsy findings in patients with severe COVID-19 pneumonia.

	Entire COVID-19 cohort	Immediate cause of death (autopsy)		
		Thrombosis or bleeding	Right cardiac failure	Sepsis
Characteristics	*n* = 11	*n* = 5	*n* = 3	*n* = 3
Pulmonary SARS-CoV-2 RNA, log_{10} copies/ml, median (IQR)	2.46 (1.73–3.81)	2.24 (0.87–3.48)	2.46 (1.73–6.06)	2.74 (1.25–5.90)
Sex, *n* (%)				
Female	5 (45)	1 (20)	1 (33)	3 (100)
Male	6 (55)	4 (80)	2 (67)	0 (0)
Age, years, median (IQR)	68 (62–79)	68 (62–74)	79 (71–90)	68 (45–79)
Time to death, days, median (95% CI)	19 (16–22)	19 (15–23)	26 (5–46)	19 (11–27)
Number of comorbidities, median (IQR)	5 (4–5)	5 (4–7)	4 (3–5)	5 (4–5)
Co-infection[a], *n* (%)	9 (82)	4 (80)	2 (67)	3 (100)
Chronic respiratory conditions[b], *n* (%)	7 (64)	4 (80)	2 (67)	1 (33)
Chronic cardiac conditions[c], *n* (%)	8 (73)	5 (100)	2 (67)	1 (33)
Chronic vascular conditions[d], *n* (%)	9 (82)	3 (60)	3 (100)	3 (100)
Chronic renal conditions, *n* (%)	2 (18)	1 (20)	0 (0)	1 (33)
Chronic gastrointestinal conditions[e], *n* (%)	5 (45)	2 (40)	1 (33)	2 (67)
Chronic endocrine conditions[f], *n* (%)	3 (27)	2 (40)	0 (0)	1 (33)
Autoimmune diseases[g], *n* (%)	1 (9)	1 (20)	0 (0)	0 (0)
Chronic haematological conditions, *n* (%)	0 (0)	0 (0)	0 (0)	0 (0)
History of solid neoplasia[h], *n* (%)	2 (18)	2 (40)	0 (0)	0 (0)
Anticoagulation, *n* (%)	8 (73)	4 (80)	2 (67)	2 (67)
Antibiotic treatment, *n* (%)	11 (100)	5 (100)	3 (100)	3 (100)
ICU (invasive ventilation, ECMO, HD), *n* (%)	9 (82)	4 (80)	2 (67)	3 (100)
ES frequency, median (IQR)	2 (1–6)	2 (1.5–4.5)	6 (0–13)	2 (0–11)
TS frequency, median (IQR)	0 (0–0)	0 (0–1)	0 (0–0)	0 (0–0)
FFP frequency, median (IQR)	0 (0–14)	0 (0–16)	0 (0–0)	5 (0–27)
Microthrombi, autopsy proof, *n* (%)	9 (82)	4 (80)	2 (67)	3 (100)
ARDS, autopsy proof of DAD, *n* (%)	9 (82)	4 (80)	3 (100)	2 (67)
Pulmonary abscesses, autopsy proof, *n* (%)	3 (27)	0 (0)	0 (0)	3 (100)

SARS-CoV-2, severe acute respiratory syndrome coronavirus 2; log, logarithm; RNA, ribonucleic acid; *n*, number of patients; IQR, interquartile range; CI, confidence interval; ICU, intensive care unit; ECMO, extracorporeal membrane oxygenation; HD, haemodialysis; ES, erythrocyte substitution concentrate; TS, thrombocyte substitution concentrate; FFP, fresh frozen plasma; ARDS, acute respiratory distress syndrome; DAD, diffuse alveolar damage; HIV, human immunodeficiency virus; HSV-1, herpes simplex virus 1.

[a] Co-infection included bacterial (*Pseudomonas aeruginosa*, *Staphylococcus epidermidis*, *Staphylococcus aureus*, *Enterococcus faecium*), viral (HIV, HSV-1), and fungal (*Candida* species) pathogens.

[b] Respiratory conditions comprised chronic obstructive pulmonary disease, asthma, and obstructive sleep apnoea syndrome.

[c] Cardiac conditions comprised cardiac insufficiency, chronic ischemic heart disease, hypertensive heart disease, and persistent arrhythmias.

[d] Vascular conditions comprised arterial hypertension, atherosclerosis, and peripheral arterial occlusive disease.

[e] Gastrointestinal conditions comprised liver cirrhosis and peptic ulcer.

[f] Endocrinological conditions comprised diabetes mellitus type II, hypothyreosis, and dyslipoproteinemia.

[g] Autoimmune disease was rheumatoid arthritis.

[h] Solid neoplasia comprised history of squamous cell lung cancer or basal cell carcinoma.

injuries who were matched for age. The median time from death to autopsy was comparable in the two groups ($p = 0.6$), namely 3 days in the COVID-19 patients (interquartile range (IQR) 1–5 days) versus 2 days in the control cohort (IQR 1–3.5 days). The clinical characteristics and causes of death with COVID-19 are shown in Table 1 and Figure 1.

Histopathology of bone marrow and spleen of COVID-19 patients

To characterize the morphology of the bone marrow and spleen of COVID-19 patients, a histopathological assessment in comparison to non-COVID-19 controls was performed (Figures 2 and 3). Bone marrow from the vertebral bodies was available for all patients. Splenic tissue was obtained from 10 COVID-19 deceased patients and three control patients.

Seventy-three percent ($n = 8$) of COVID-19 patients presented with hypercellularity and an increase in immature myelopoiesis with precursors in the bone marrow. Moreover, megakaryopoiesis was increased in COVID-19 patients, with a maximum value of 17 megakaryocytes/HPF as compared to 9 megakaryocytes/HPF in control patients. Bone marrow megakaryocytes of COVID-19 patients showed signs of immaturity with cell diameters of <20 μm and hypolobulated nuclei in 55% ($n = 6$). Peripheral or visceral microthrombi were found in 82% ($n = 9$) of COVID-19 cases but were absent in the control cohort.

CD34- and CD117-positive cells were <5% in the bone marrow of both COVID-19 and control patients.

Of alls COVID-19 patients, 55% (n = 6) showed mild fibrosis of the bone marrow medullary space, which was not present in the control cohort. As a correlate of monocytic activity, variability of monocytic and macrophage cell shapes (round vs stellar-shaped) was observed in 82% ($n = 9$) of COVID-19 patients. However, after EDTA decalcification, the macrophage iron load was weak and signs of hemophagocytosis were absent.

A substantial decrease of the white pulp was observed in the spleen of all COVID-19 decedents but not in the control cohort. CD34+ cells were <5% in all splenic samples. As compared to the bone marrow, a moderate intracellular macrophage iron load was found in 40% ($n = 4$) of COVID-19 spleens, which was paired with a thickening of the splenic capsule and the trabecular arterioles and therefore interpreted as a sign of chronic blood retention due to right cardiac insufficiency.

COVID-19 is associated with severe B cell loss in bone marrow and spleen

After the basic assessment, the lymphatic components of the bone marrow and spleen were evaluated. Strikingly, a severe loss of B cells with a subsequent CD20+ B cell depletion in either bone marrow or spleen was observed in 64% of COVID-19 patients ($n = 7$).

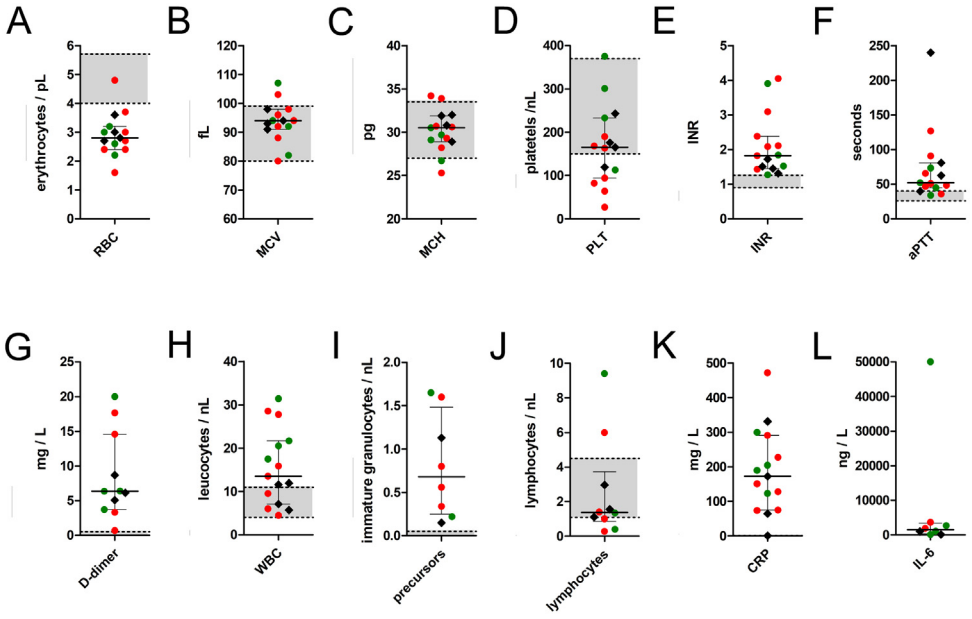

Figure 1. Ante-mortem laboratory findings from peripheral blood samples that were drawn within the week prior to death from 11 patients with COVID-19 as compared to those of the four control patients.
Note: Red dots represent findings in COVID-19 patients with B cell depletion in either spleen or bone marrow ($n = 7$), green dots represent findings in COVID-19 patients with B cell preservation ($n = 4$), black hashes represent findings in the control cohort ($n = 4$). Centre values represent the median of the entire cohort ($n = 15$) and error bars indicate the standard deviation of the pooled values. The upper and lower normal limits for each value are charted as grey zones.
Abbreviations and conversion factors: RBC, red blood cell count; MCV, median corpuscular volume; MCH, median corpuscular haemoglobin; PLT, platelets; INR, international normalized ratio (prothrombin time ratio between patient sample and standard sample); aPTT, activated partial thromboplastin time; WBC, white blood cell count; CRP, C-reactive protein (multiply by 9.5238 to convert to nmol/l); IL-6, interleukin 6.

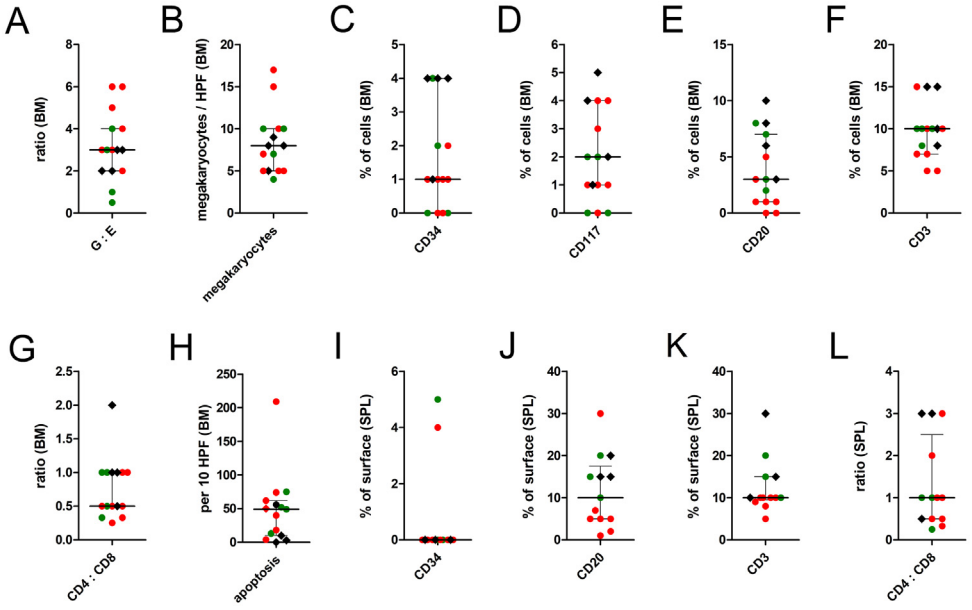

Figure 2. Post-mortem histopathological findings in the bone marrow and in the spleen tissue of 11 COVID-19 deceased patients as compared to four control patients.
Note: Red dots represent findings in COVID-19 patients with B cell depletion in either spleen or bone marrow ($n = 7$), green dots represent findings in COVID-19 patients with B cell preservation ($n = 4$), black hashes represent findings in the control cohort ($n = 4$). Centre values represent the median of the entire cohort ($n = 15$) and error bars indicate the standard deviation of the pooled values.
Abbreviations: G:E, granulocytopoiesis to erythrocytopoiesis ratio.

In the group of patients with B cell loss, CD20+ B cell counts were $\leq$1% in the bone marrow and 1–5% in the spleen (Figure 3). Of these patients, three had combined B cell loss in both bone marrow and spleen, whereas two had either isolated B cell loss in the bone marrow or in the spleen. Moreover, plasma cell depletion was observed in four out of five patients who had CD20+ B cell loss in the bone marrow. These changes were absent in the control cohort.

Although complete CD20+ B cell loss was not observed in the remaining four COVID-19 decedents, CD20+ B cell counts were still lower than in the control cohort. More precisely, median CD20+ B

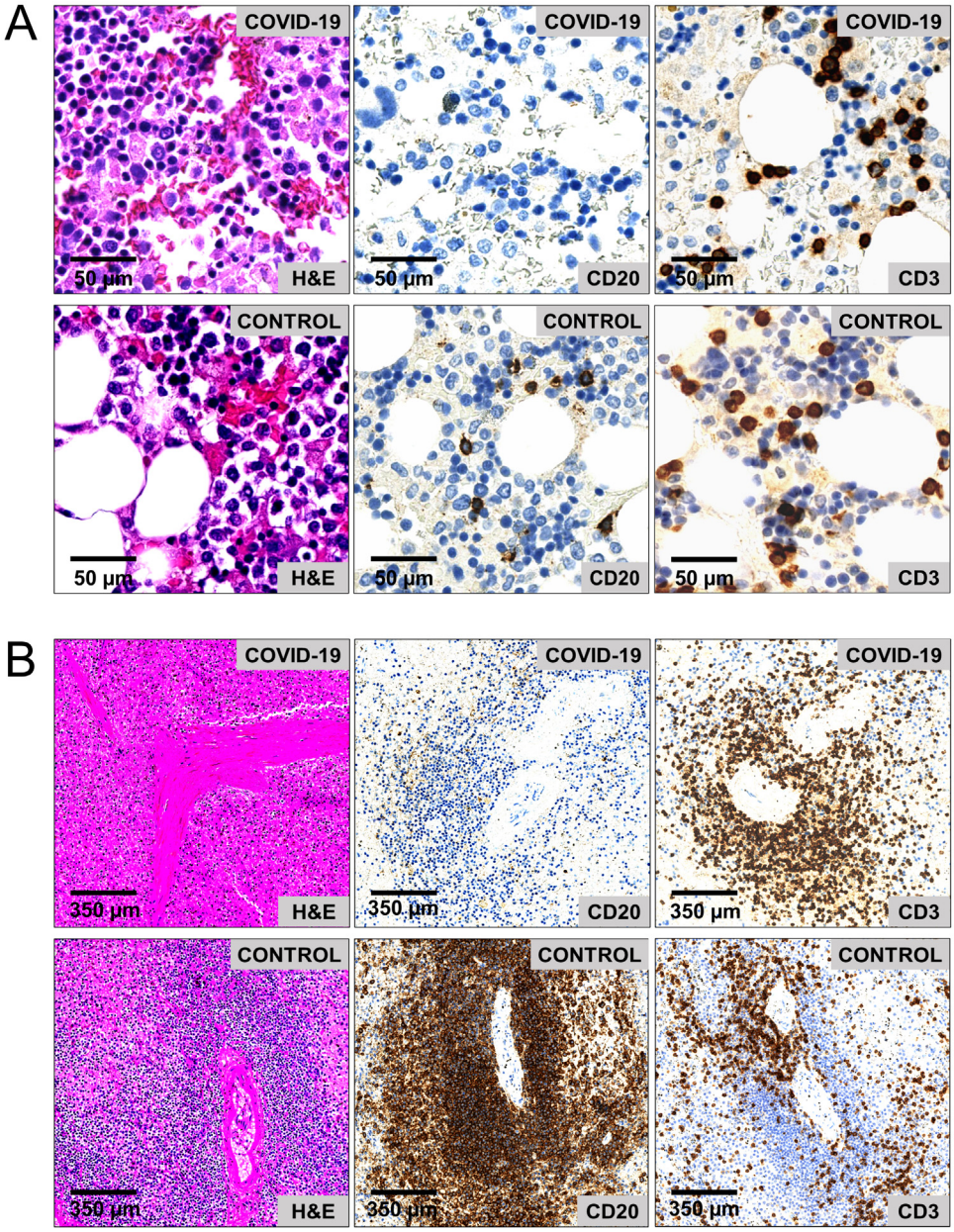

Figure 3. CD20+ B cell loss in a COVID-19 deceased patient (age 79 years) as compared to a control patient (age 78 years). (A) Histopathology of cell-rich areas in the bone marrow show immaturity of myelopoiesis (left row), severe loss of CD20+ B cells (middle row), and a stabilized CD3+ T cell count (right row) in the COVID-19 patient as compared to the control patient. (B) Histopathology of the spleen shows atrophy of peri-arteriolar white pulp (left row), caused by loss of CD20+ B cells (middle row); the peri-arteriolar CD3+ T cell distribution is regular (right row).
Abbreviations: HPF, high power field; H&E, haematoxylin and eosin; BM, bone marrow; SPL, spleen.

cell counts were 2% in the bone marrow and 5% in the spleen within the COVID-19 cohort, as compared to 7% and 15% in the control cohort (Figure 2). In COVID-19 patients with B cell preservation, the remaining B cells had a tendency towards mixed nodular aggregation (n = 4).

Quite contrary to the severe loss of B cells, T cell counts were marginally decreased in the bone marrow of COVID-19 patients (median 10%) as compared to the control cohort (median 12.5%). In the bone marrow, the maximum T cell/B cell ratio was 10:0 in COVID-19 patients as compared to 3:1 in the control samples. Comparable effects of only slight T cell reduction in the spleen were observed (Figures 2K and 3). T cell subpopulations were skewed towards a CD8+ phenotype with CD4/CD8 ratios of on average 1:2 (range 1:1–1:4) in COVID-19 patients as compared to 1:1 (range 2:1–1:1) in the bone marrow of the control cohort. Of note, one of the COVID-19 patients had an HIV co-infection and received antiretroviral therapy.

Next, an analysis was conducted to determine whether severe B cell loss in COVID-19 patients was linked to the viral SARS-CoV2 burden or determined by a specific clinical risk profile. Interestingly, a tendency towards a higher SARS-CoV-2 RNA load was observed in pulmonary tissue of patients with complete B cell loss, particularly when the bone marrow was affected. Although median viral copy numbers were approximately equal in both groups (Table 2), maximum viral copy numbers of nearly 800,000 and 1,150,000/10,000 cells in patients with total B cell loss as compared to 6500/10,000 cells in patients with B cell preservation were observed.

In order to identify a possible B cell EBV reactivation during parallel SARS-CoV-2 infection, EBER-ISH was performed on all

Table 2
Characteristics of 11 patients with severe COVID-19 pneumonia and B cell loss or B cell preservation in the bone marrow or spleen.

Characteristics of the COVID-19 cohort (n = 11)	Severe B cell loss (n = 7)	B cell preservation (n = 4)
Pulmonary SARS-CoV-2 RNA level, log_{10} copies/ml, median (IQR)	2.46 (1.73–5.90)	2.69 (1.49–3.64)
Age, years, median (IQR)	71 (68–79)	65 (61–76)
Time to death, days, median (95% CI)	19 (6–32)	19 (16–22)
Number of comorbidities, median (IQR)	4 (3–5)	5 (5–5)
Viral co-infection, n (%)	1 (14)	1 (25)
Bacterial co-infection, n (%)	3 (43)	3 (75)
Fungal co-infection, n (%)	1 (14)	1 (25)
HIV, n (%)	1 (14)	0 (0)
Autoimmune disease, n (%)	0 (0)	1 (25)
History of solid malignancy, n (%)	2 (30)	0 (0)
ICU (invasive ventilation, ECMO, HD), n (%)	6 (86)	3 (75)
Sepsis, n (%)	5 (71)	3 (75)
Pulmonary abscesses, autopsy proof, n (%)	2 (30)	1 (25)
ARDS with autopsy proof of DAD, n (%)	5 (71)	4 (100)

SARS-CoV-2, severe acute respiratory syndrome coronavirus 2; log, logarithm; RNA, ribonucleic acid; n, number of patients; IQR, interquartile range; CI, confidence interval; ICU, intensive care unit; ECMO, extracorporeal membrane oxygenation; HD, haemodialysis; ARDS, acute respiratory distress syndrome.

bone marrow specimens, combined with additional PCR clarification. Both techniques revealed an absence of EBV. Clinical characteristics were equally distributed between COVID-19 patients with and without B cell loss (p-values >0.5 in all pairwise comparisons). Moreover, intervals from onset of symptoms to death were heterogeneous in both groups (Table 2).

Signs of sepsis-acquired immunodeficiency after severe bacterial superinfection of viral COVID-19 pneumonia

Autopsy revealed sepsis due to abscess-forming pneumonia in 27% (n = 3) of COVID-19 patients (Figure 4). Of these patients, one belonged to the group with B cell loss and two were in the group with B cell preservation. Clinically, these patients were in septic shock prior to death and either swabs or pulmonary lavage showed bacterial superinfection of the underlying COVID-19 pneumonia with *Staphylococcus aureus*, *Staphylococcus epidermidis*, or *Pseudomonas aeruginosa*. To determine whether sepsis-related immunosuppression had been present prior to death in these three patients, an additional immunological characterization of the bone marrow microenvironment was performed by grading immunohistochemical expression of B and T cell markers, HLA-DR, caspase 3, and PD-L1 in relation to pulmonary SARS-CoV-2 levels and intervals from onset of symptoms to death (Figure 4). Immunohistochemistry revealed signs of sepsis-acquired immunodeficiency in the bone marrow that were reflected morphologically by an increase in bone marrow cellularity and immature myeloid cell types with multiple myeloid precursors. Furthermore, an increase

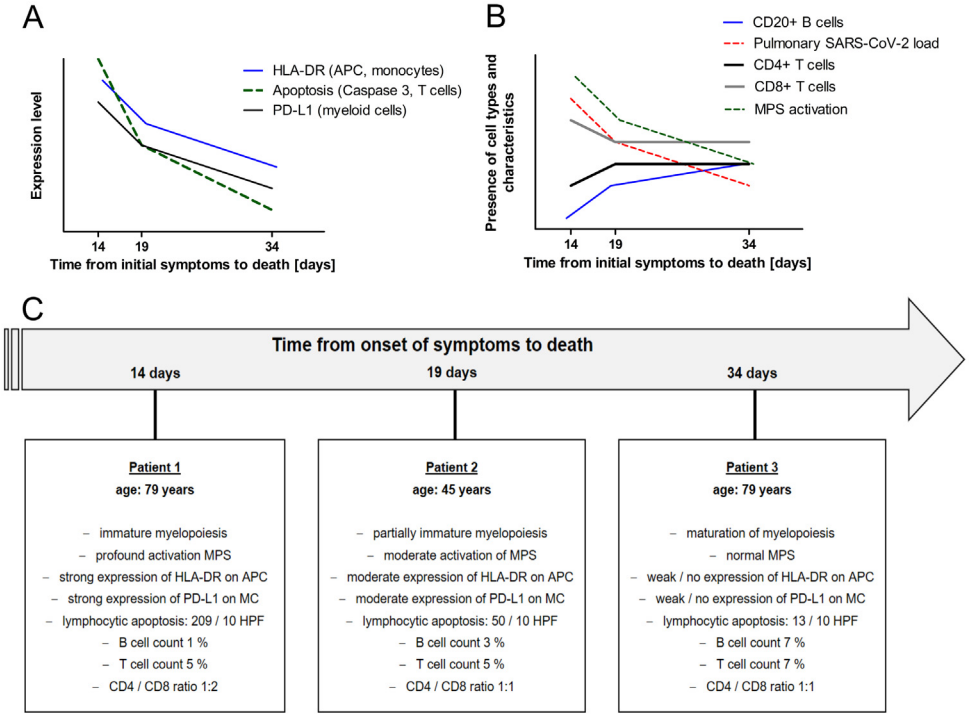

Figure 4. Signs of sepsis-acquired immunodeficiency and relative development of bone marrow morphology according to the interval from onset of symptoms to death in three COVID-19 deceased patients with abscess-forming superinfection of viral pneumonia. (A) Expression levels of immunological markers, (B) cell types and presence of morphological characteristics, (C) morphological results of bone marrow evaluation in each patient.
Abbreviations: HLA-DR, human leukocyte antigen DR isotype; APC, antigen-presenting cells; PD-L1, programmed death ligand 1; SARS-CoV-2, severe acute respiratory syndrome coronavirus 2; MPS, monocyte–macrophage system; MC, myeloid cells; HPF, high-power field.

in T cell apoptosis with more than 200 apoptosis per 10 HPF (characterized by caspase 3) and an increase in neutrophilic PD-L1 expression were observed in the two patients with fulminant sepsis and early death. These changes were combined with an early loss of B cells and an increase in pulmonary SARS-CoV-2 levels. Furthermore, we observed a continuous decrease in monocytic activation with transition from numerous round-shaped CD68-positive monocytes in the bone marrow of these two patients with early death as compared to fewer stellar-shaped CD68-positive macrophages in the patient who died later. The latter was accompanied by a decrease in HLA-DR expression on monocytes, macrophages, and dendritic cells, especially in the patient with prolonged sepsis.

Discussion

This study gives a detailed insight into the morphology of bone marrow and splenic tissue reactions in COVID-19 decedents. This appears to be the first study to examine the specific role of bone marrow B cells in the context of COVID-19-associated lymphocytopenia. Furthermore, information is provided on the sepsis-related pathophysiology in patients with COVID-19 pneumonia with pulmonary bacterial co-infection.

Confirmatory to recent COVID-19 autopsy reports, thromboembolic events, bleeding, right cardiac failure, and sepsis with abscess-forming pneumonia and consecutive severe pulmonary damage were observed as immediate causes of death (Bryce et al., 2020; Elezkurtaj et al., 2020; Lax et al., 2020; Wichmann et al., 2020). The median age of the study cohort was 68 years and thus comparable to that of COVID-19 decedents reported in other studies (Bryce et al., 2020; Zhou et al., 2020). Since thromboembolic events, bleeding, or sepsis were present in the vast majority (73%) of patients, COVID-19-associated changes in hematopoietic tissue were of particular interest here.

As a correlate of hyperinflammation, recent studies have reported excessive macrophage stimulation and signs of consecutive hemophagocytosis in the bone marrow of a subset of COVID-19 patients (Bryce et al., 2020; Merad and Martin, 2020). Consistent with an acute-phase reaction, hypercellularity and predominantly immature granulopoiesis with multiple myeloid precursors were observed in the bone marrow, mirrored by a release of immature granulocytes and anemia in the peripheral blood (Figures 1 and 2). Furthermore, regenerating megakaryopoiesis was found, which probably resulted from thromboembolic events that were present in 82% of the study cohort, and this could be explained by hyperinflammation-associated endothelial dysfunction (Bryce et al., 2020; Varga et al., 2020). In turn, the latter might have contributed as a mediator for the release of immature granulocytes or myeloid suppressor cells to the periphery via microscopic rupture of the endothelial barrier in the bone marrow (Venet et al., 2020).

Hemophagocytosis was not present in the study cohort. Instead, signs of incipient sepsis-acquired immunodeficiency were found in the bone marrow of patients with severe bacterial superinfection of COVID-19 pneumonia. This was reflected by an early increase in myeloid PD-L1 expression, lymphocytic apoptosis, and macrophage anergy with loss of antigen-presenting capacity (Hotchkiss and Nicholson, 2006; Huang et al., 2014; Landelle et al., 2010). Usually, sepsis-acquired immunodeficiency is accompanied by cytokine-related T cell exhaustion, the release of myeloid suppressor cells, and epigenetically determined monocyte switch to endotoxin tolerance after bacterial stress (Biswas and Lopez-Collazo, 2009; Boomer et al., 2011; Cheng et al., 2016; Lorente-Sorolla et al., 2019). Thus, methylation-related predisposition for immune memory adaption may influence the highly variable outcome and affect later immunity in patients with severe bacterial co-infection of COVID-19 pneumonia to a varying extent. However, due to the limited number of cases, these findings need to be interpreted with caution.

Apart from immunodeficiency, severe lymphocytopenia in the peripheral blood has been reported as an adverse risk factor for the clinical outcome of COVID-19 patients (Chen et al., 2020; Tan et al., 2020; Terpos et al., 2020; Zheng et al., 2020) and there is increasing evidence that this is caused by a follicular atrophy in lymphoid organs (Bryce et al., 2020; Buja et al., 2020; Kaneko et al., 2020; Lax et al., 2020). A recent study by Kaneko et al. indicated a crucial impact of tumour necrosis factor alpha (TNF-α) that leads to early blockage of B cell lymphoma 6 protein (BCL6)-positive T helper cells with a consecutive loss of BCL6-positive germinal centre B cells in early stages of COVID-19, and therefore to a dysregulation of the humoral immune response (Kaneko et al., 2020). In the present study, severe lymphocytopenia was consistently observed in the peripheral blood, in the spleen, and even in the bone marrow of more than half of the COVID-19 cohort, which was combined with a release of immature granulocytes, elevated C-reactive protein, and increased interleukin 6 levels in the peripheral blood (Figure 1I–L). This suggested an ongoing acute phase reaction but an inadequate specific immune response in these patients.

Unfortunately, peripheral B/T cell counts were not available for the study cohort of COVID-19 decedents. However, in the spleen and in the bone marrow, the severe loss of lymphocytes was predominantly caused by a depletion of B cells rather than by a loss of T cells (Figure 2E, F, J, L). Therefore, the findings strongly emphasize a separate involvement of B cells in the pathogenesis of COVID-19, since viral sepsis usually results in a significant decrease of both CD4+ T cells and CD20+ B cells (Hotchkiss et al., 2001). In the subgroup of patients with severe B cell loss, pulmonary SARS-CoV-2 levels were exceedingly high, and a distinct clinical risk profile was absent as compared to patients with B cell preservation (Table 2). Hence, SARS-CoV-2-associated effects were the most probable link towards the observed B cell loss, although the relatively small sample size precluded the detection of statistically significance differences between the two groups. Furthermore, it should be mentioned that B cell counts in the bone marrow are generally low, with median values ranging from 2% to 5% in the literature (Fauci, 1975) and 7% in the control cohort of the present study. Nevertheless, the co-occurrence of both loss of B cells and loss of plasma cells allows for the assumption of an excessive activation of B cell-specific pathways such as the B cell transforming growth factor beta (TGF-β) pathway (Chua et al., 2020; Islam et al., 1991). The latter seems reasonable, since a recent study by Biasi et al. reports a significant loss of naïve and mature B cells accompanied by an expansion of immunoglobulin M+ plasmablasts in the peripheral blood of patients with COVID-19 pneumonia (De Biasi et al., 2020). In analogy to therapy-induced B cell depletion under treatment with rituximab, systemic immunoglobulin therapy might be helpful in the subset of COVID-19 patients with severe B cell loss.

In conclusion, the study findings indicate that infection with SARS-CoV-2 is related to mechanisms of sepsis-acquired immunodeficiency, as well as B cell and plasma cell depletion in hematopoietic tissues. Since B cells and plasma cells are major key players of acquired immunity, the study findings add further explanation to the limited durability of the humoral immune response to SARS-CoV-2 (Kaneko et al., 2020; Long et al., 2020) and thus contribute to the pathophysiological understanding of COVID-19.

Funding

We acknowledge support from the German Research Foundation (DFG) and the Open Access Publication Fund of Charité - Universitätsmedizin Berlin.

Ethical approval

The study was performed in accordance with local ethics guidelines (institutional ethics committee approval EA2/066/20) and the Declaration of Helsinki. Written consent was obtained from all next of kin.

Conflict of interest

All authors declare no conflict of interest with regard to this work.

Author contributions

JI, DH, AvB, and SE designed the study. EM, SG, JI, HR, JM, FM, HH, SE, and DH performed autopsies and tissue sampling. JI, VH, AL, FM, HH, DH, AvB, and SE performed histopathology and laboratory workup. VC performed SARS-CoV2-PCR testing. JI, EM, SG, JW, and LB collected and interpreted clinical data. JI and SG performed the statistical analysis. DH, AvB, and SE supervised the study. All authors wrote, revised, and approved the manuscript.

Acknowledgements

We gratefully thank Anistan Sebastiampillai, Juliane Plaschke, and Franziska Egelhofer for their excellent technical support during the autopsy procedure. Furthermore, we thank Julia Scheider, Sebastian Brünink, and Tobias Bleicker for their help with SARS-CoV-2 RT-PCR testing.

References

Ackermann M, Verleden SE, Kuehnel M, Haverich A, Welte T, Laenger F, et al. Pulmonary vascular endothelialitis, thrombosis, and angiogenesis in Covid-19. NEJM 2020;383(2):120–8, doi:http://dx.doi.org/10.1056/NEJMoa2015432.

Biswas SK, Lopez-Collazo E. Endotoxin tolerance: new mechanisms, molecules and clinical significance. Trends Immunol 2009;30(10):475–87, doi:http://dx.doi.org/10.1016/j.it.2009.07.009.

Boomer JS, To K, Chang KC, Takasu O, Osborne DF, Walton AH, et al. Immunosuppression in patients who die of sepsis and multiple organ failure. JAMA 2011;306(23):2594–605, doi:http://dx.doi.org/10.1001/jama.2011.1829.

Bryce C, Grimes Z, Pujadas E, Ahuja S, Beasley MB, Albrecht R, et al. Pathophysiology of SARS-CoV-2: targeting of endothelial cells renders a complex disease with thrombotic microangiopathy and aberrant immune response. The Mount Sinai COVID-19 autopsy experience. medRxiv 2020;(May):20099960, doi:http://dx.doi.org/10.1101/2020.05.18.20099960.

Buja LM, Wolf DA, Zhao B, Akkanti B, McDonald M, Lelenwa L, et al. The emerging spectrum of cardiopulmonary pathology of the coronavirus disease 2019 (COVID-19): report of 3 autopsies from Houston, Texas, and review of autopsy findings from other United States cities. Cardiovasc Pathol 2020;48:107233, doi:http://dx.doi.org/10.1016/j.carpath.2020.107233.

CDC. Collection and Submission of Postmortem Specimens from Deceased Persons with Known or Suspected COVID-19. Interim Guidance of the Center for Disease Prevention and Control; 2020. https://www.cdc.gov/coronavirus/2019-ncov/hcp/guidance-postmortem-specimens.html.

Chen T, Wu D, Chen H, Yan W, Yang D, Chen G, et al. Clinical characteristics of 113 deceased patients with coronavirus disease 2019: retrospective study. BMJ (Clin Res ed) 2020;368:, doi:http://dx.doi.org/10.1136/bmj.m1091 m1091-m.

Cheng SC, Scicluna BP, Arts RJ, Gresnigt MS, Lachmandas E, Giamarellos-Bourboulis EJ, et al. Broad defects in the energy metabolism of leukocytes underlie immunoparalysis in sepsis. Nat Immunol 2016;17(4):406–13, doi:http://dx.doi.org/10.1038/ni.3398.

Chua RL, Lukassen S, Trump S, Hennig BP, Wendisch D, Pott F, et al. COVID-19 severity correlates with airway epithelium–immune cell interactions identified by single-cell analysis. Nat Biotechnol 2020;38(August (8)):970–9, doi:http://dx.doi.org/10.1038/s41587-020-0602-4.

De Biasi S, Tartaro DL, Meschiari M, Gibellini L, Bellinazzi C, Borella R, et al. Expansion of plasmablasts and loss of memory B cells in peripheral blood from COVID-19 patients with pneumonia. Eur J Immunol 2020;50:1283–94, doi:http://dx.doi.org/10.1002/eji.202048838.

Elezkurtaj S, Greuel S, Ihlow J, Michaelis E, Bischoff P, Kunze CA, et al. Causes of death and comorbidities in patients with COVID-19. medRxiv 2020;(June):20131540, doi:http://dx.doi.org/10.1101/2020.06.15.20131540.

Fauci AS. Human bone marrow lymphocytes. I. Distribution of lymphocyte subpopulations in the bone marrow of normal individuals. J Clin Invest 1975;56(1):98–110, doi:http://dx.doi.org/10.1172/JCI108085.

Faust JS, del Rio C. Assessment of deaths from COVID-19 and from seasonal influenza. JAMA Intern Med 2020;180(8):1045–6, doi:http://dx.doi.org/10.1001/jamainternmed.2020.2306.

Hotchkiss RS, Nicholson DW. Apoptosis and caspases regulate death and inflammation in sepsis. Nat Rev Immunol 2006;6(11):813–22, doi:http://dx.doi.org/10.1038/nri1943.

Hotchkiss RS, Tinsley KW, Swanson PE, Schmieg RE, Hui JJ, Chang KC, et al. Sepsis-induced apoptosis causes progressive profound depletion of B and CD4 T Lymphocytes in humans. J Immunol 2001;166(11):6952, doi:http://dx.doi.org/10.4049/jimmunol.166.11.6952.

Huang X, Chen Y, Chung C-S, Yuan Z, Monaghan SF, Wang F, et al. Identification of B7-H1 as a novel mediator of the innate immune/proinflammatory response as well as a possible myeloid cell prognostic biomarker in sepsis. J Immunol 2014;192(3):1091, doi:http://dx.doi.org/10.4049/jimmunol.1302252.

Islam KB, Nilsson L, Sideras P, Hammarström L, Smith CI. TGF-beta 1 induces germline transcripts of both IgA subclasses in human B lymphocytes. Int Immunol 1991;3(11):1099–106, doi:http://dx.doi.org/10.1093/intimm/3.11.1099.

Iuliano AD, Roguski KM, Chang HH, Muscatello DJ, Palekar R, Tempia S, et al. Estimates of global seasonal influenza-associated respiratory mortality: a modelling study. Lancet 2018;391(10127):1285–300, doi:http://dx.doi.org/10.1016/S0140-6736(17)33293-2.

Kaneko N, Kuo HH, Boucau J, Farmer JR, Allard-Chamard H, Mahajan VS, et al. Loss of Bcl-6-expressing T follicular helper cells and germinal centers in COVID-19. Cell 2020;183(October (1)), doi:http://dx.doi.org/10.1016/j.cell.2020.08.025 143-157.e13.

Landelle C, Lepape A, Voirin N, Tognet E, Venet F, Bohé J, et al. Low monocyte human leukocyte antigen-DR is independently associated with nosocomial infections after septic shock. Intensive Care Med 2010;36(11):1859–66, doi:http://dx.doi.org/10.1007/s00134-010-1962-x.

Lax SF, Skok K, Zechner P, Kessler HH, Kaufmann N, Koelblinger C, et al. Pulmonary arterial thrombosis in COVID-19 with fatal outcome: results from a prospective, single-center, clinicopathologic case series. Ann Intern Med 2020;, doi:http://dx.doi.org/10.7326/M20-2566.

Levi M, Thachil J, Iba T, Levy JH. Coagulation abnormalities and thrombosis in patients with COVID-19. Lancet Haematol 2020;7(6):e438–40, doi:http://dx.doi.org/10.1016/S2352-3026(20)30145-9.

Long Q-X, Liu BZ, Deng H-J, Wu G-C, Deng K, Chen Y-K, et al. Antibody responses to SARS-CoV-2 in patients with COVID-19. Nat Med 2020;26(6):845–8, doi:http://dx.doi.org/10.1038/s41591-020-0897-1.

Lorente-Sorolla C, Garcia-Gomez A, Català-Moll F, Toledano V, Ciudad L, Avendaño-Ortiz J, et al. Inflammatory cytokines and organ dysfunction associate with the aberrant DNA methylome of monocytes in sepsis. Genome Med 2019;11(1):66, doi:http://dx.doi.org/10.1186/s13073-019-0674-2.

Merad M, Martin JC. Pathological inflammation in patients with COVID-19: a key role for monocytes and macrophages. Nat Rev Immunol 2020;20(6):355–62, doi:http://dx.doi.org/10.1038/s41577-020-0331-4.

Tan L, Wang Q, Zhang D, Ding J, Huang Q, Tang Y-Q, et al. Lymphopenia predicts disease severity of COVID-19: a descriptive and predictive study. Sig Transduc Target Ther 2020;5(1):33, doi:http://dx.doi.org/10.1038/s41392-020-0148-4.

Terpos E, Ntanasis-Stathopoulos I, Elalamy I, Kastritis E, Sergentanis TN, Politou M, et al. Hematological findings and complications of COVID-19. Am J Hematol 2020;95(July (7)):834–47, doi:http://dx.doi.org/10.1002/ajh.25829.

Tzankov A, Dirnhofer S, Beham-Schmid C. Normal bone marrow and common reactive alterations. Pathologe 2012;33(6):496–507, doi:http://dx.doi.org/10.1007/s00292-012-1649-x.

Varga Z, Flammer AJ, Steiger P, Haberecker M, Andermatt R, Zinkernagel AS, et al. Endothelial cell infection and endotheliitis in COVID-19. Lancet 2020;395(10234):1417–8, doi:http://dx.doi.org/10.1016/S0140-6736(20)30937-5.

Venet F, et al. Myeloid cells in sepsis acquired immunodeficiency. Ann NY Acad Sci 2020;, doi:http://dx.doi.org/10.1111/nyas.14333.

WHO. Coronavirus Disease (COVID-19) Situation Report of the World Health Organization—Weekly Epidemiological Update. 2020. https://www.who.int/docs/default-source/coronaviruse/situation-reports/20200811-covid-19-sitrep-204.pdf?sfvrsn=1f4383dd_2.

Wichmann D, Sperhake J-P, Lütgehetmann M, Steurer S, Edler C, Heinemann A, et al. Autopsy findings and venous thromboembolism in patients with COVID-19: a prospective cohort study. Ann Intern Med 2020;173:268–77, doi:http://dx.doi.org/10.7326/M20-2003.

Wölfel R, Corman VM, Guggemos W, Seilmaier M, Zange S, Müller MA, et al. Virological assessment of hospitalized patients with COVID-2019. Nature 2020;581(7809):465–9, doi:http://dx.doi.org/10.1038/s41586-020-2196-x.

Zheng H-Y, Zhang M, Yang C-X, Zhang N, Wang X-C, Yang X-P, et al. Elevated exhaustion levels and reduced functional diversity of T cells in peripheral blood may predict severe progression in COVID-19 patients. Cell Mol Immunol 2020;17(5):541–3, doi:http://dx.doi.org/10.1038/s41423-020-0401-3.

Zhou F, Yu T, Du R, Fan G, Liu Y, Liu Z, et al. Clinical course and risk factors for mortality of adult inpatients with COVID-19 in Wuhan, China: a retrospective cohort study. Lancet 2020;395(10229):1054–62, doi:http://dx.doi.org/10.1016/S0140-6736(20)30566-3.